Persistence of RNAi-Mediated Knockdown in *Drosophila* Complicates Mosaic Analysis Yet Enables Highly Sensitive Lineage Tracing

Justin A. Bosch, Taryn M. Sumabat, and Iswar K. Hariharan[1]
Department of Molecular and Cell Biology, University of California, Berkeley, California 94720

ABSTRACT RNA interference (RNAi) has emerged as a powerful way of reducing gene function in *Drosophila melanogaster* tissues. By expressing synthetic short hairpin RNAs (shRNAs) using the Gal4/UAS system, knockdown is efficiently achieved in specific tissues or in clones of marked cells. Here we show that knockdown by shRNAs is so potent and persistent that even transient exposure of cells to shRNAs can reduce gene function in their descendants. When using the FLP-out Gal4 method, in some instances we observed unmarked "shadow RNAi" clones adjacent to Gal4-expressing clones, which may have resulted from brief Gal4 expression following recombination but prior to cell division. Similarly, Gal4 driver lines with dynamic expression patterns can generate shadow RNAi cells after their activity has ceased in those cells. Importantly, these effects can lead to erroneous conclusions regarding the cell autonomy of knockdown phenotypes. We have investigated the basis of this phenomenon and suggested experimental designs for eliminating ambiguities in interpretation. We have also exploited the persistence of shRNA-mediated knockdown to design a sensitive lineage-tracing method, i-TRACE, which is capable of detecting even low levels of past reporter expression. Using i-TRACE, we demonstrate transient infidelities in the expression of some cell-identity markers near compartment boundaries in the wing imaginal disc.

KEYWORDS RNAi; shRNA; Gal4/UAS; lineage tracing; compartment boundary

RNA interference (RNAi) is an endogenous gene-silencing mechanism in eukaryotic cells that has been harnessed as a powerful reverse genetics tool (Hannon 2002). RNAi is initiated by short interfering RNAs (siRNAs) or microRNAs (miRNAs) that target messenger RNAs for degradation or translational inhibition in a sequence-specific manner (Wilson and Doudna 2013). Importantly, RNAi can be artificially induced by gene-specific hairpin RNAs that are processed into siRNAs (Fire *et al.* 1998; Paddison *et al.* 2002). These RNAi reagents, along with completely sequenced genomes, have enabled experimenters to perform loss-of-function studies in diverse organisms (Mohr *et al.* 2014).

An important consideration for knockdown experiments is whether RNAi-mediated knockdown is sustained or transient. In *Caenorhabditis elegans* (Sijen *et al.* 2001) and plants (Vaistij *et al.* 2002), siRNAs undergo amplification by RNA-dependent RNA polymerases (RdRPs), leading to a long-lasting RNAi response. In contrast, *Drosophila* and vertebrates do not have RdRP homologs (Zong *et al.* 2009) and RNAi is normally transient (Chi *et al.* 2003; Roignant *et al.* 2003). The development of transgenic strategies to express RNA hairpins has overcome this problem, and RNAi can be induced, sustained, and/or repressed using different promoter sequences (Perrimon *et al.* 2010; Livshits and Lowe 2013). This ability to control RNAi in a temporal manner *in vivo* has proven essential for generating reversible phenotypes (Livshits and Lowe 2013) and for dissecting the biological functions of pleiotropic genes (Perrimon *et al.* 2010).

In *Drosophila*, accurate control of where and when RNAi occurs is critical for evaluating the effects of knockdown in specific cell populations *in vivo* (Perrimon *et al.* 2010). Spatiotemporal control of RNAi-mediated knockdown is most often accomplished using the Gal4/*UAS* system (Fischer *et al.* 1988; Brand and Perrimon 1993), where cell/tissue-specific Gal4 transgenes drive co-expression of hairpin RNAs and cellular markers (*e.g.*, *UAS-GFP*) under *UAS* control. These hairpin

doi: 10.1534/genetics.116.187062
Manuscript received January 14, 2016; accepted for publication March 9, 2016; published Early Online March 15, 2016.
Available freely online through the author-supported open access option.
Supplemental material is available online at www.genetics.org/lookup/suppl/doi:10.1534/genetics.116.187062/-/DC1.
[1]Corresponding author: University of California, 361 LSA, Berkeley, CA 94720. E-mail: ikh@berkeley.edu

transgenes are available either as long double-stranded RNAs (dsRNAs) or as short hairpin RNAs (shRNAs) embedded within a *miR-1* microRNA backbone (Perrimon *et al.* 2010), with the latter thought to be more effective at gene silencing (Ni *et al.* 2011). Gal4 transgenes are also used as reporters of endogenous gene expression (Fischer *et al.* 1988; Brand and Perrimon 1993), and, for many Gal4 lines, expression may dynamically change on a timescale of hours or days during development (Yeh *et al.* 1995; Evans *et al.* 2009), homeostasis (Micchelli and Perrimon 2006; Buchon *et al.* 2009), or environmental changes (Halfon *et al.* 1997; Agaisse *et al.* 2003). Several studies in mammalian cell culture and *in vivo* models have shown that protein levels do not recover immediately after turning off RNAi, usually requiring >2 days (Gupta *et al.* 2004; Dickins *et al.* 2005; Bartlett and Davis 2006; Zhang *et al.* 2007; Baccarini *et al.* 2011). Despite the known potential for RNAi persistence to occur, no studies to date have documented or addressed how this can affect Gal4-regulated knockdown experiments that require precise temporal and spatial resolution *in vivo*.

Here, we demonstrate in *Drosophila* tissues that even transient production of shRNAs leads to persistent gene knockdown after Gal4 expression has ceased. We show that this phenomenon can, in the context of common experimental designs, lead to false interpretations about the identity of cells undergoing knockdown, and we provide experimental workarounds to address this issue. Furthermore, we exploit RNAi persistence to develop a novel lineage-tracing tool called i-TRACE that we demonstrate can be used to identify instances where even brief changes in gene expression have occurred during the generation of specific cell lineages.

Materials and Methods

Drosophila genetics

Crosses were maintained on standard fly food at 25° unless otherwise noted.

Most transgenic stocks were obtained or derived from the Bloomington Stock Center and are listed here with corresponding stock numbers (BL#): *ptc-Gal4* (BL2017), *en-Gal4* (BL30564), *dpp-Gal4* (BL1553), *nub-Gal4* (BL25754), *ap-Gal4* (BL3041), *UAS-GFP* (BL6874), *UAS-RFPnls* (BL30556), *UAS-mCD8.ChRFP* (BL27391), *UAS-GFP-shRNA#1* Chr. II (BL41557), *UAS-GFP-shRNA#1* Chr. III (BL41556), *UAS-GFP-dsRNA* (BL9330), *UAS-RFP-shRNA* (BL35785), *UAS-crb-shRNA* (BL40869), *UAS-crb-dsRNA* (BL27697), *hsp70-GFP* (BL51354), *ubi-GFPnls* (BL5189), *ubi-RFPnls* (BL34500), *UAS-Nslmb-vhhGFP4* (BL38421), *tub-Gal80ts* (BL7108), *G-TRACE* (BL28281), *hsFLP* (BL8862), *Act5c-FRT-CD2-FRT-Gal4* (BL4780), and *Act5c-FRT-y+-FRT-Gal4* (BL3953). Additional stocks with BL#s are listed in Table S1 and Table S2.

The remaining stocks used originated from the publications noted: *ci-Gal4* (Croker *et al.* 2006), *hh-Gal4* (Tanimoto *et al.* 2000), *esg-Gal4* (Micchelli and Perrimon 2006), *FRT40A* MARCM (Lee and Luo 1999), and *FRT40A* (Xu and Rubin 1993).

For experiments involving FLP-out Gal4 induction of shRNAs in clones (Figure 1; Supplemental Material, Figure S1), different combinations of transgenes produce shadow RNAi clones (genotypes written as Chr. X; Chr. II; Chr. III): *GFP* RNAi (Figure 1B; Figure S1, B and C); *hsFLP/+*; *ubi-GFP/+*; *Act5c-FRT-CD2-FRT-Gal4*, *UAS-RFP/UAS-GFP-shRNA*; *RFP* RNAi (Figure S1, A, D, and F); *hsFLP/+*; *Act5c-FRT-y+-FRT-Gal4*, *UAS-GFP/ubi-RFP*; *UAS-RFP-shRNA/+*; *crb* RNAi (Figure 1, C and D); and *hsFLP/+*; *+/+*; *Act5c-FRT-CD2-FRT-Gal4*, *UAS-GFP/UAS-crb-shRNA*.

For experiments involving knockdown of different genes using the *ptc-Gal4* RNAi persistence tester (Figure S3, Table S2), the following crossing scheme was used: *yv*; *UAS-gene-shRNA* (Chr. III) X *w*; *ptc-Gal4, UAS-GFP, ubi-RFP; UAS-RFP-shRNA*.

For i-TRACE analysis of *enhancer-Gal4* lines, the following crossing schemes were used: *enhancer-Gal4* X *w*; *UAS-RFP, ubi-GFP; UAS-GFP-shRNA*; and *enhancer-Gal4* X *w*; *UAS-GFP, ubi-RFP; UAS-RFP-shRNA*. iTRACE tester stocks will be made available through the Bloomington Stock Center.

Dissections, antibody staining, and microscopy

Unless otherwise noted, all tissues were dissected with forceps in glass well dishes with 1× PBS. Tissues were fixed in 4% paraformaldehyde in 1× PBS for 20 min. After washing in 1× PBS, tissues were stained with DAPI (1 ng/μl) in 1× PBS for 1 hr, washed with 1× PBS, and mounted onto slides with Vectashield mounting media (Vector Labs) or SlowFade Gold mounting medium (Life Technologies). Mounted samples were imaged on a Zeiss 700 or 780 confocal microscope. Confocal slices were processed with ImageJ software (NIH).

For wing imaginal discs, wandering third instar larvae were bisected and inverted to expose the imaginal discs to fixative. For immunostaining of wing discs, fixed carcasses with attached wing discs were permeabilized with PBS+0.1% Triton-X100 for 20 min, blocked with PBS+0.1% Triton-X100+5% normal goat serum for 1 hr, and incubated with primary antibodies diluted in blocking solution overnight at 4°. Samples were washed three times in PBS+0.1% Triton-X100 for 15 min each. Subsequent steps involving staining using secondary antibodies were the same as primary antibodies. Antibodies used were the following: mouse anti-Arm (1:100, N2 7A1; Developmental Studies Hybridoma Bank) and rat anti-Crb (1:500) (Richard *et al.* 2006).

For adult midguts, females ~1 week post eclosion were starved for 4 hr to purge any gut contents that are autofluorescent. This was performed by placing adults into empty vials containing filter paper soaked with 4% sucrose. Adult midguts were dissected from decapitated animals by gently pulling out the gut and placing it into fixative.

For experiments requiring heat-shock induction of the *hs-FLP* transgene in wing imaginal discs, ~72 hr after egg deposition larvae were placed in a 37° water bath for 15–30 min (for FLP-out Gal4 experiments) or 1–2 hr (for MARCM experiments) and returned to 25°. Larvae were dissected as wandering third instar larvae.

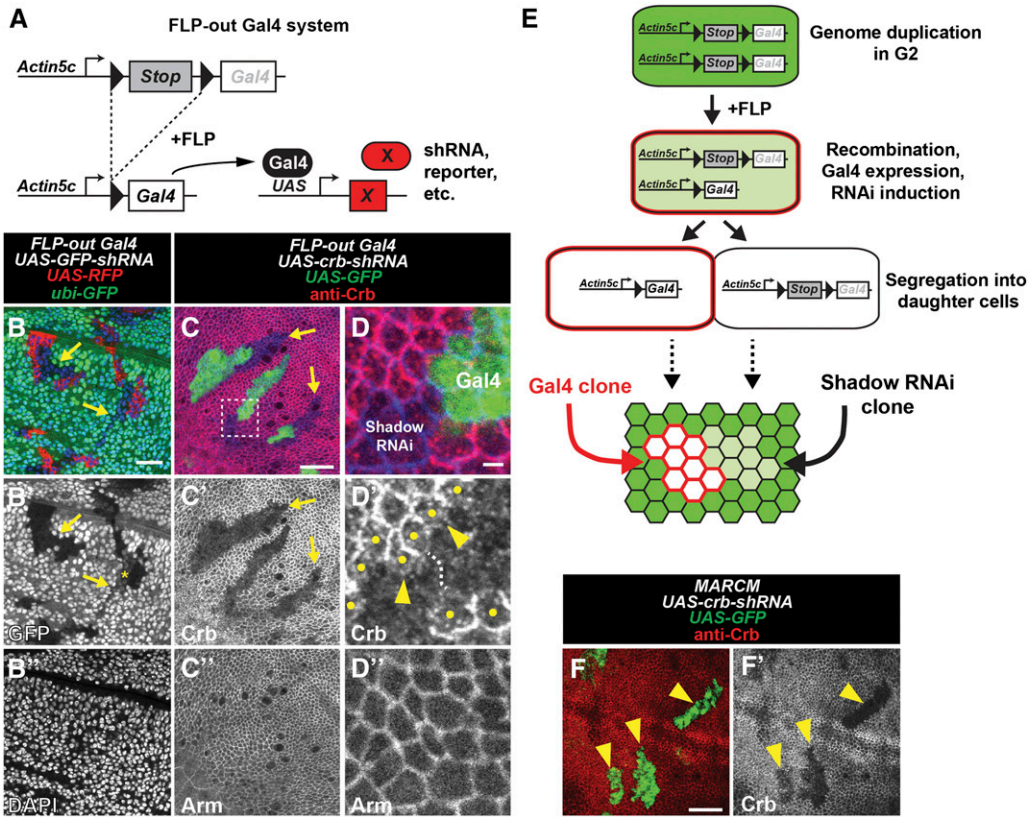

Figure 1 Gene knockdown in shadow RNAi clones when using the FLP-out Gal4 system. (A) Genetic diagram of the FLP-out Gal4 system. The *Actin5c* promoter drives constitutive expression of Gal4 after FLP/*FRT* recombination. (B–D) FLP-out Gal4 clones in the wing imaginal disc. (B) Gal4 clones express RFP (red) and *GFP-shRNA* and knockdown GFP (green). Shadow RNAi clones knock down GFP but do not express RFP (arrows). Asterisk in B′ indicates shadow RNAi clone with intermediate levels of knockdown. Cell nuclei labeled with DAPI (blue). Bar, 20 μm. (C) Gal4 clones express GFP (green) and *crb-shRNA* and knockdown Crb protein (red). Shadow RNAi clones knock down Crb protein (arrows). Arm staining (blue) shows cell membrane. Bar, 20 μm. (D) Magnification of region in C. Arrowheads indicate that Crb protein is missing on the membrane of wild-type cells (dots) that contact Gal4 and shadow RNAi cells. Bar, 2 μm. (E) Model for generation of shadow RNAi clones. Prior to cell division, recombination during G2 causes expression of Gal4 (red) and knockdown of target gene expression (green). Following cell division, target gene knockdown persists in non-Gal4-expressing cells (shadow RNAi clone). (F) MARCM Gal4 clones in the wing disc (arrowheads). Gal4 clones express GFP (green) and *crb-shRNA* and knock down Crb protein (red). Bar, 20 μm. All panels with (′) or (′′) designation show isolated greyscale channels of the merged image in their respective parental panel.

For experiments requiring heat-shock induction of the *hsp70-GFP* transgene, crosses were incubated at 37° for 30 min, returned to 25°, and dissected 2 hr later. Non-heat-shocked controls were kept at 25° until dissection.

For heat-shift experiments involving *tub-Gal80ts*, eggs from crosses were initially incubated at 18° (permissive temperature, Gal4 off). Vials were incubated at 29° (non-permissive temperature, Gal4 on) for 16 hr until dissected as wandering third instar larvae. Controls were kept at the same temperature throughout development (18° or 29°).

Data availability

The authors state that all data necessary for confirming the conclusions presented in the article are represented fully within the article.

Results

Transient expression of shRNAs causes persistent knockdown in unmarked "shadow RNAi" cells

The FLP-out Gal4 system (Pignoni and Zipursky 1997) can be used to induce RNAi in a clonal lineage of cells that stably express Gal4. Clones are generated using a heat-shock-inducible FLP transgene, which catalyzes the removal of a transcriptional stop upstream of the Gal4-coding sequence (Figure 1A). While using this system, we unexpectedly found that clonal expression of shRNAs causes knockdown in cells that do not express Gal4. For example, in larvae that ubiquitously express GFP (*ubi-GFP*), we generated Gal4 clones that express shRNA targeting GFP (*UAS-GFP-shRNA*) and red fluorescent protein (*UAS-RFP*) and dissected wing discs 48 hr after clone induction (ACI). As expected, RFP-expressing clones knock down GFP (Figure 1B). However, we also observed patches of cells that knock down GFP but do not express RFP. We refer to this unexpected cell type as "shadow RNAi" cells since these cells exhibit knockdown of their target gene but do not express Gal4 as assessed by the absence of RFP expression.

Importantly, we find that shadow RNAi cells are produced when shRNAs target two other genes, *ubi-RFP* (Figure S1A) and the endogenous gene *crumbs* (*crb*) (Figure 1, C and D). Furthermore, *crb* shadow RNAi cells exhibited a known *crb* mutant phenotype characterized by altered localization of Crb where they contact wild-type cells (Figure 1D) (Pellikka *et al.* 2002; Chen *et al.* 2010; Hafezi *et al.* 2012). In addition, shadow RNAi cells were readily observed in other larval tissues (Figure S1, B–D) and using independently derived transgenes (see *Materials and Methods*). These results suggest that production of shadow RNAi cells may be an inherent phenomenon when using the FLP-out Gal4 system, as

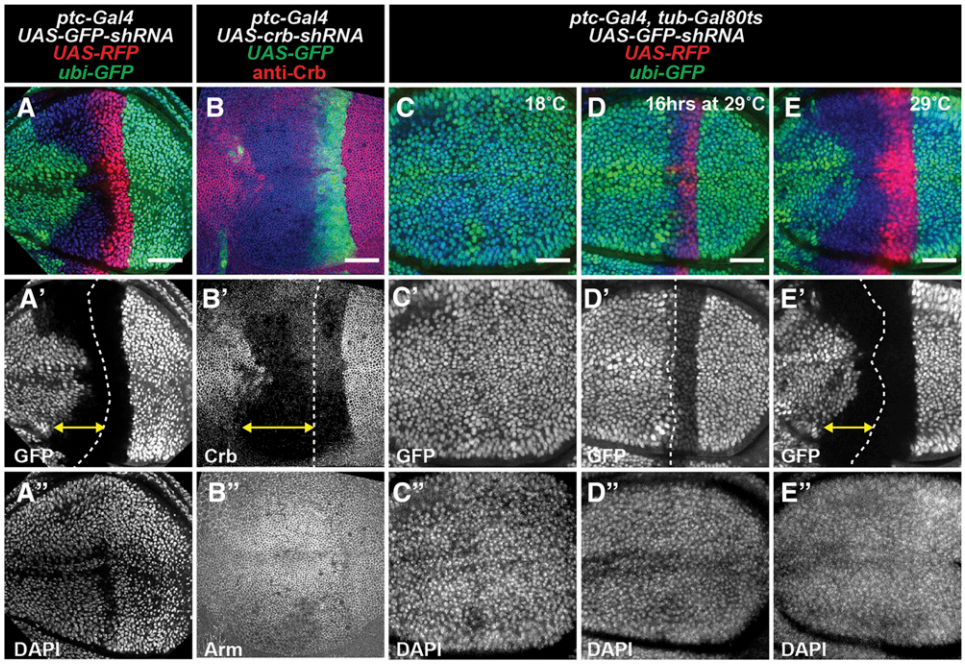

Figure 2 Gene knockdown in shadow RNAi cells caused by dynamic expression of *ptc-Gal4*. (A–E) Wing imaginal discs with RNAi under control of *ptc-Gal4*. (A) *ptc-Gal4* expression of RFP (red) and *GFP-shRNA* cause knockdown of GFP (green). Cell nuclei labeled with DAPI (blue). (B) *ptc-Gal4* expression of GFP (green) and *crb-shRNA* cause knockdown of Crb protein (red). Arm staining (blue) shows cell membrane. (C–E) Temperature control of *ptc-Gal4* expression with *tub-Gal80^{ts}*. *ptc-Gal4* expression of RFP (red) and *GFP-shRNA* cause knockdown of GFP (green). Cell nuclei labeled with DAPI (blue). (C) Larvae always kept at 18°. (D) Larvae shifted from 18° to 29° 16 hr before dissection. (E) Larvae always kept at 29°. Double arrow in A′, B′, and E′ indicates RNAi persistence in cells anterior to the *ptc* stripe. Bars, 50 μm. All panels with (′) or (′′) designation show isolated greyscale channels of the merged image in their respective parental panel.

opposed to sporadic effects such as chromosomal instability or epigenetic silencing of transgenes.

We note that tests of three other endogenous genes (*fat*, *gigas*, and *dachshund*) did not obviously generate shadow RNAi cells (Table S1; not shown). In addition, when we repeated FLP-out Gal4 experiments using dsRNAs targeting GFP (*UAS-GFP-dsRNA*), we found that shadow RNAi cells were not clearly visible and may have exhibited only weak knockdown (Figure S1E). Therefore, shadow RNAi cells may manifest only when targeting particular genes or when using certain RNAi reagents (see *Discussion*).

Several observations of shadow RNAi cells hint at a mechanism by which they are generated. Shadow RNAi cells nearly always appear as cohesive groups in contact with Gal4 clones (Figure 1, B and C, Figure S1), which is a well-documented behavior of sister clones in the imaginal disc (Xu and Rubin 1993). Furthermore, in cases where shadow RNAi cells exhibit partial knockdown of the target gene (Figure 1B), each cell within a cohesive group shows the same level of knockdown, suggesting a synchronized reversal of RNAi over time. Indeed, we find that knockdown in shadow RNAi cells is barely visible at 72 hr ACI (Figure S1F), suggesting that knockdown is not sustained as in Gal4-expressing clones. These observations suggest that shadow RNAi cells produced using the FLP-out Gal4 system are a sister lineage to Gal4 clones and that knockdown persists for up to 3 days after being transiently induced.

To explain our observations with the FLP-out Gal4 system, we propose that shRNAs are transiently expressed in an ancestral mother cell that gave rise to Gal4-expressing clones and sister shadow RNAi clones. This event could occur during G2 when cells have duplicated their genome if one of two *Act-FRT-stop-FRT-Gal4* transgenes undergoes recombination and briefly expresses Gal4 before cell division (Figure 1E). In contrast, recombination during G1, or recombination of both *Act-FRT-stop-FRT-Gal4* transgenes, would not be expected to generate shadow RNAi clones. To test this model, we performed clonal RNAi experiments using the MARCM (Mosaic Analysis with a Repressible Cell Marker) system, which restricts Gal4 activity until after two daughter cells are produced and the levels of the Gal80 repressor in the cytoplasm decay (Lee and Luo 1999). Consistent with this hypothesis, when using MARCM to express shRNAs that target *crb*, we find that Crb protein is knocked down only in the Gal4 clone (Figure 1F). In addition, this result rules out the possibility that shRNAs or Gal4 are transferred from the Gal4 clone into shadow RNAi clones.

Since our model predicts that transient expression of shRNAs causes persistence of RNAi-mediated knockdown, we wanted to verify this using an independent method. *patched-Gal4* (*ptc-Gal4*) is a commonly used enhancer trap line that expresses Gal4 in the *ptc* expression pattern (Hinz *et al.* 1994). In early wing disc development, *ptc-Gal4* is expressed in all cells of the anterior compartment and later becomes restricted to a thin stripe of anterior cells that border the posterior compartment (Phillips *et al.* 1990; Evans *et al.* 2009). When we used *ptc-Gal4* to express shRNAs targeting *GFP* (Figure 2A) or *crb* (Figure 2B), we observed knockdown of the target gene within cells of the stripe currently expressing Gal4, as well as cells far anterior to the stripe that no longer express Gal4 (assessed by a fluorescent protein expressed under UAS control). In contrast, dsRNAs targeting *GFP* transcript or a nanobody fusion that degrades GFP protein (Caussinus *et al.* 2012) cause knockdown of GFP fluorescence mainly within the *ptc*-expressing stripe, although some cells immediately anterior to the stripe have

reduced GFP levels (Figure S2, B and C). Similarly, dsRNAs that target *crb* cause knockdown only within the *ptc*-expressing stripe (Figure S2D). To directly test if past expression of *ptc-Gal4* in more anterior regions of the wing disc is required to generate shadow RNAi cells, we used a temperature-sensitive Gal80 transgene (McGuire *et al.* 2003) to restrict expression of Gal4 to a 16-hr window immediately preceding dissection (Figure 2D). Under these conditions, shadow RNAi cells are not observed, suggesting that the shadow RNAi cells were generated by prior expression of the shRNA in those cells.

Investigation of mechanisms contributing to the persistence of RNAi-mediated knockdown

Our observation that it takes ~3 days to reverse the effects of GFP knockdown is consistent with reports in mammalian cell culture and *in vivo* mouse models (Gupta *et al.* 2004; Dickins *et al.* 2005; Bartlett and Davis 2006; Zhang *et al.* 2007; Baccarini *et al.* 2011), although our experiments were performed at a comparably lower temperature (25°). In these mammalian systems, it is generally thought that reversal from RNAi occurs by siRNA degradation and/or dilution with cell divisions (Dickins *et al.* 2005; Baccarini *et al.* 2011). Yet, considering this explanation, we were surprised by the high degree of persistent GFP knockdown following a short pulse of shRNA expression (Figure 1, B–D). Therefore, we considered the possibility that RNAi was being actively maintained in some manner.

Active maintenance of RNAi has been demonstrated in different species, such as RNAi amplification in *C. elegans* (Sijen *et al.* 2001; Alder *et al.* 2003) or RNAi-induced transcriptional silencing (RITS) (Verdel *et al.* 2004) in *S. pombe*. In addition, Piwi-interacting RNAs (piRNAs) target transcripts via an amplifying "ping-pong" cycle (Brennecke *et al.* 2007). Initiation of each of these mechanisms requires the presence of target transcripts. Therefore, we tested whether RNAi persistence in *Drosophila* tissues occurs when the target gene is not expressed until immediately before dissection. This was accomplished using a heat-shock-inducible GFP transgene (*hs-GFP*) that is highly expressed when animals are incubated at 37° (Figure 3). Using *ptc-Gal4* to express *GFP-shRNA* in a *hs-GFP* background, and inducing GFP expression 2 hr before dissection, we find that GFP knockdown occurs in the *ptc* stripe (RFP+) as well as in cells far anterior (RFP−) (Figure 3C). We do not detect GFP fluorescence without heat shock and observe tissue autofluorescence only at higher exposure settings (Figure 3B′). These results suggest that previous expression of transcripts is not required for RNAi persistence in shadow RNAi cells.

We also systematically tested the requirement of genes that might promote RNAi persistence based on mechanisms that operate in other systems. This was accomplished by knocking down each gene while monitoring transient knockdown of a ubiquitously expressed RFP (*ubi-RFP*) using the *ptc-Gal4* expression system. Our goal was to identify genes that are selectively required for RNAi persistence in

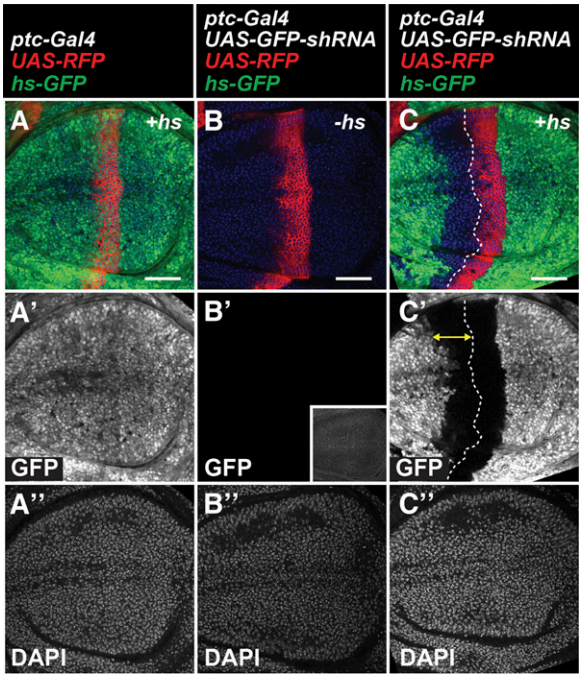

Figure 3 RNAi persistence does not require past expression of target transcripts. (A–C) Wing imaginal discs with *ptc-Gal4* expression of RFP (red). All discs contain the *hs-GFP* transgene. GFP (green) expression is induced with a heat shock (hs) 2 hr before dissection. Cell nuclei labeled with DAPI (blue). (A) Heat-shock induction of GFP (green) with no *GFP-shRNA*. (B) Expression of *GFP-shRNA* with no heat shock. (B′) Inset shows maximum exposure. (C) Expression of *GFP-shRNA* with heat shock. Double arrow in C′ indicates RNAi persistence in cells anterior to the *ptc* stripe. Bars, 50 μm. All panels with (′) or (″) designation show isolated greyscale channels of the merged image in their respective parental panel.

cells anterior to the *ptc* stripe. We tested *Drosophila* orthologs of genes involved in RITS, chromatin-remodeling genes, and machinery involved in miRNA, siRNA, and piRNA processing. With one exception, none of the genes when knocked down abolished persistent RNAi of the *ubi-RFP* reporter gene (Figure S3; Table S2). The exception was *Ago2* RNAi, which nearly abolishes RFP knockdown in all cells expressing *ptc-Gal4* (Figure S3C). This result is consistent with the known role of Ago2 to bind siRNAs and coordinate RNAi-induced silencing complex (RISC) degradation of target transcripts (Ni *et al.* 2011). In summary, our results favor a model where the persistence of RNAi is simply the result of a slow rate of degradation of shRNAs and/or their siRNA derivatives.

i-TRACE: a novel lineage analysis tool based on RNAi

Since even transient expression of an shRNA could generate persistent knockdown (Figure 1, B and C), we explored its use as a lineage-tracing tool. To facilitate RNAi-based lineage tracing with Gal4 lines, we constructed a fly strain containing three transgenes: (1) a reporter of Gal4 activity (*e.g.*, *UAS-RFP*), (2) a ubiquitously expressed target gene (*e.g.*, *ubi-GFP*), and (3) a Gal4-controlled shRNA (*e.g.*, *UAS-GFP-shRNA*) (Figure 4A). Therefore, when this triple-transgenic line is crossed

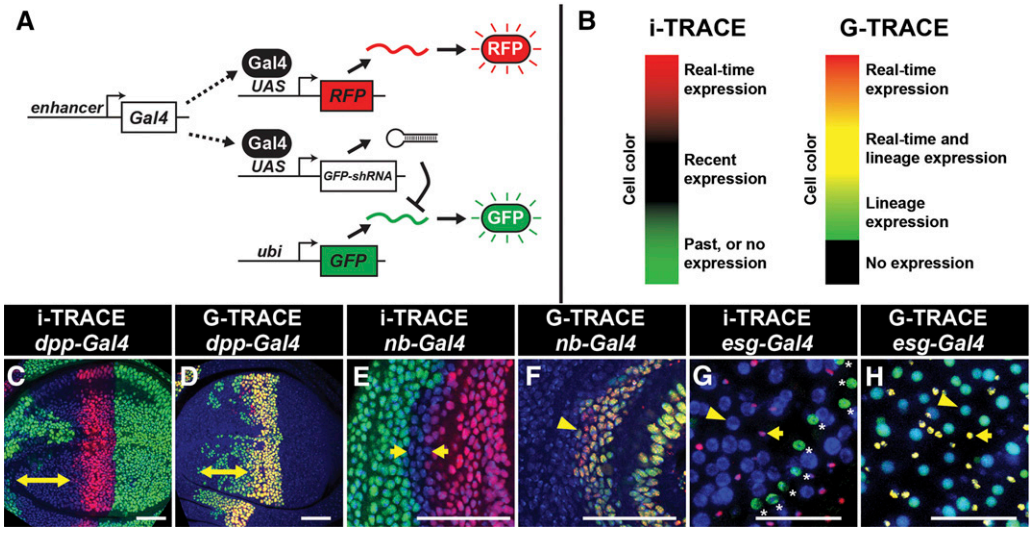

Figure 4 The i-TRACE system. (A) Diagram of the genetic components that form the i-TRACE system. Enhancer-driven expression of Gal4 induces RFP and *GFP-shRNA* in cells. *GFP-shRNA* targets ubiquitously expressed GFP transcripts from *ubi-GFP*. (B) A comparison of cell color representations between the i-TRACE and G-TRACE systems. (C–H) Analysis of enhancer-Gal4 expression with i-TRACE and G-TRACE. Cell nuclei labeled with DAPI (blue). Bars, 50 μm. (C and D) *dpp-Gal4* expression in the wing imaginal disc. Double arrows indicate RNAi persistence in C, or recombined lineage in D, in cells anterior to the *ptc* stripe. (E and F) *nb-Gal4* expression in the wing imaginal disc. (E) Arrows indicate region of past expression at outer edge of pouch. (F) Arrowhead indicates outer boundary of *nb-Gal4* expression. (G and H) *esg-Gal4* expression in the adult midgut. Arrows indicate RFP+ nuclei; arrowheads indicate enterocyte nuclei. Asterisks in G indicate overlying muscle nuclei with GFP expression.

with a Gal4 line, F_1 progeny will contain cells and tissues that report real-time Gal4 expression (RFP+, GFP−) and recent Gal4 expression (RFP−, GFP−) (Figure 4B). Since exogenous fluorescent transgenes are used, the tissues being analyzed are wild type and antibody staining is not necessary. We refer to this system as i-TRACE (RNA**i**-**T**echnique for **R**eal-time **A**nd **C**lonal **E**xpression), which shares a similar naming convention with G-TRACE, a recombination-based lineage-tracing technique (Evans *et al.* 2009). We compared i-TRACE with G-TRACE using several well-characterized Gal4 lines.

dpp-Gal4 expresses in the anterior wing disc at early developmental stages and becomes restricted to a thin stripe of cells at the border between anterior and posterior compartments (Masucci *et al.* 1990; Evans *et al.* 2009). Using i-TRACE, we observed large regions of the anterior wing disc that previously expressed *dpp-Gal4* (Figure 4C). Using G-TRACE (Figure 4D), we find that the region of lineage-traced cells is patchier and restricted to a smaller domain. Results with *ptc-Gal4* are comparable to *dpp-Gal4* as they express in similar domains (Figure S4). *nubbin-Gal4* (*nub-Gal4*) expresses in the wing disc pouch, and the outer edge of this domain is thought to shift throughout larval development (Zirin and Mann 2007). Using i-TRACE, we confirmed this phenomenon by finding a thin ring of cells outside of the *nub-Gal4* domain that previously expressed Gal4 (Figure 3E). In contrast, when using G-TRACE, this ring of past expression is not visible (Figure 3F). Thus, in at least these two cases, i-TRACE appears more sensitive than G-TRACE.

escargot-Gal4 (*esg-Gal4*) expresses in two cell types of the adult midgut: intestinal stem cells and their immediate descendants called enteroblasts (EBs) (Micchelli and Perrimon 2006). EBs give rise to two differentiated cell types that no longer express *esg-Gal4*: enterocytes and enteroendocrine cells. Together, these four cell types compose the entire midgut epithelium. Using i-TRACE with *esg-Gal4*, we observed that all cells of the midgut are GFP− (Figure 3G). These cells include enterocytes, which are discernible by their large nuclear size (Micchelli and Perrimon 2006). In contrast, muscle cells that surround the midgut epithelium express GFP, confirming that animals contain the *ubi-GFP* transgene. This result supports the model that differentiated cell types in the midgut epithelium are descendants of a lineage that expressed *esg-Gal4*. Using G-TRACE with *esg-Gal4* demonstrates similar results to i-TRACE (Figure 3H).

In summary, our analysis of several Gal4 lines using the i-TRACE system suggests that it is a useful tool for simultaneously visualizing past and present gene expression.

Reversible changes in compartment identity markers are revealed using i-TRACE

During animal development, boundaries between gene expression domains are important to physically separate cells of different function (Dahmann *et al.* 2011). In the *Drosophila* wing disc, four compartments are separated by two boundaries, the anterior/posterior (A/P) boundary, and the dorsal/ventral (D/V) boundary (Figure 5A). The A/P boundary is specified during embryogenesis and the D/V boundary at the end of the first larval instar. Lineage-tracing techniques have demonstrated that cells initially specified in one compartment do not normally switch identities (Garcia-Bellido *et al.* 1973). We set out to test this model by analyzing the expression patterns of several compartment-specific Gal4 lines with i-TRACE.

The A/P boundary is specified by the selector gene *engrailed* (*en*) (Kornberg *et al.* 1985), which expresses in all cells of the posterior compartment and activates transcription of *hedgehog* (*hh*) (Tabata *et al.* 1992). Using i-TRACE to analyze *hh-Gal4*, we observed present expression in the

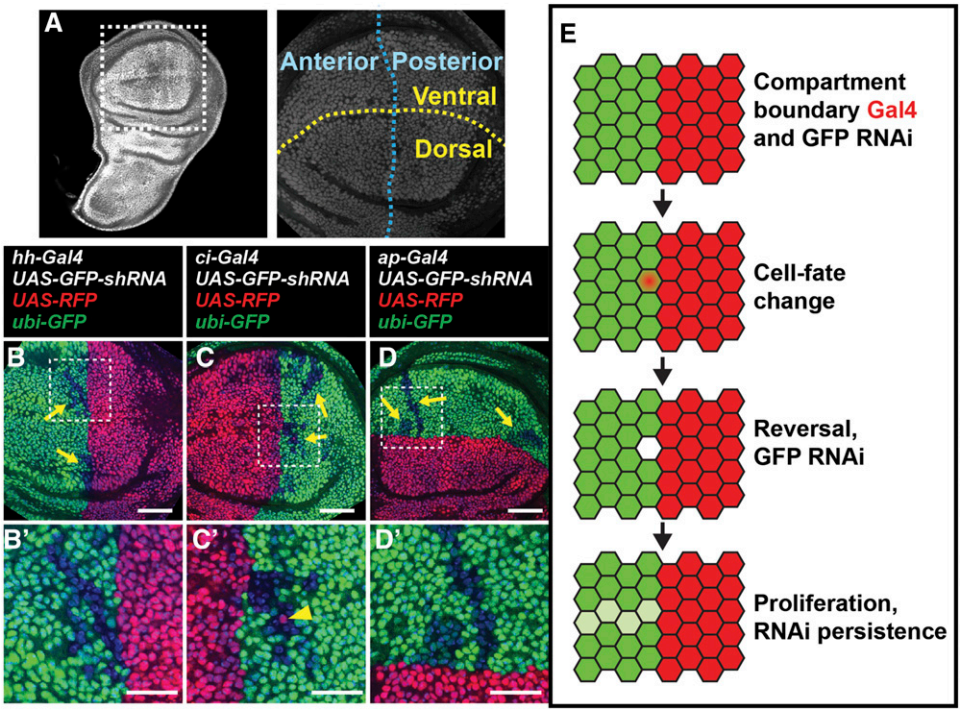

Figure 5 Reversible cell-fate switching at compartment boundaries in the wing disc. (A) Wandering third instar wing disc expressing *ubi-GFP*. Boxed area indicates magnified pouch region with overlay of compartment boundaries, ventral–dorsal (horizontal yellow line) and anterior–posterior (vertical blue line). (B–D) i-TRACE analysis of compartment-specific Gal4 lines in the wing disc. (B) *hh-Gal4* (posterior expression). (C) *ci-Gal4* (anterior expression). (D) *ap-Gal4* (dorsal expression). Cell nuclei labeled with DAPI (blue). Arrows indicate shadow RNAi cells in the opposite compartment to enhancer-Gal4 expression. Boxes indicate magnifications in B′, C′, and D′. Arrowhead in C′ indicates a posterior RFP+ cell. Bars, 50 μm in B, C, D; 25 μm in B′, C′, and D′.

posterior compartment of the third instar wing disc (Figure 5B), consistent with previous studies (Tanimoto *et al.* 2000). Surprisingly, in all discs imaged (>20), we also observed patches of shadow RNAi cells in the anterior compartment (Figure 5B), indicating that *hh-Gal4* was previously expressed in these cells. These shadow RNAi patches were always adjacent to the A/P boundary and expressed anterior identity genes (Figure S5). Furthermore, we occasionally found that a subset of anterior shadow RNAi cells actively expressed *hh-Gal4* (Figure S5, A and B; Figure S6, A and B). To verify our results via a different method, we used G-TRACE to analyze past *hh-Gal4* expression in the wing disc. Again, we find patches of cells that previously expressed *hh-Gal4* in the anterior compartment (Figure S6, C and D), although at a much lower frequency (1 disc of 10). This is consistent with the reduced sensitivity of G-TRACE in detecting past expression. These results suggest that at least some anterior cells in the wing disc express *hh-Gal4* at some point in development.

During late third instar wing development, *en* expression expands into a small region of the anterior compartment that borders the posterior compartment (Blair 1992). We wondered whether this anterior *en* expression could be responsible for activating *hh-Gal4* in anterior cells as seen with i-TRACE. To test this possibility, we examined a developmental time series to determine when anterior shadow RNAi cells form in *hh-Gal4* i-TRACE wing discs. We find that anterior *hh-Gal4* shadow RNAi cells are first visible in the second instar and early third instar (Figure S7, A–D). We also find similar results with *en-Gal4* i-TRACE (Figure S7, G–J), where the appearance of anterior shadow RNAi cells precedes the late third instar expression of *en-Gal4* in anterior cells (Figure S7, K and L). Furthermore, the anterior *en* expression domain, which extends mostly along the dorsal/ventral boundary, does not obviously overlap with the location and shape of *hh-Gal4* shadow RNAi patches (Figure S8). These results suggest that *en-Gal4* and *hh-Gal4* are expressed in anterior cells at a time point much earlier than previously described.

To determine if other markers of compartment identity transiently express outside of their canonical compartment, we analyzed the expression patterns of additional Gal4 lines with i-TRACE in the third instar wing disc. *cubitus interruptus* (*ci*), an essential component of the *hh* pathway, is repressed in the posterior compartment by *en* and thus is expressed only in the anterior compartment (Eaton and Kornberg 1990). Using i-TRACE to analyze *ci-Gal4*, we find the expected current expression in the anterior compartment, but also evidence of past expression in cells of the posterior compartment (Figure 5C). In addition, a subset of posterior shadow RNAi cells actively express *ci-Gal4* (Figure 5C′). *apterous* (*ap*) is a selector gene expressed in the dorsal compartment of the wing disc (Blair *et al.* 1994). Using i-TRACE to analyze *ap-Gal4*, we observe cells in the ventral compartment that previously expressed Gal4 (Figure 5D). In summary, our results with i-TRACE suggest that the expression of each of four different compartment-specific Gal4 lines (*hh-Gal4*, *en-Gal4*, *ci-Gal4*, and *ap-Gal4*) is not completely restricted to its specific compartment.

Several similarities in the characteristics of shadow RNAi patches produced from different compartment Gal4 lines suggest that they are clones that originate close to the compartment boundary. First, these cells appear as cohesive groups with similar levels of knockdown, suggesting that they

belong to a shared clonal lineage that underwent several cell divisions after expression of Gal4 (Xu and Rubin 1993). Second, these patches are frequently elongated in the proximo/distal direction, an indicator that there is significant proliferation after the labeling event (Baena-Lopez *et al.* 2005). Third, these patches lie in proximity to the compartment boundary defined by the particular Gal4 line. These results suggest that cells located at wing-disc compartment boundaries can transiently express at least some markers of the opposite compartment (Figure 5E).

Discussion

In this study, we show that transient expression of shRNAs in *Drosophila* tissues can cause persistent knockdown in cells that outlasts co-expressed marker transgenes. We term this effect "shadow RNAi," since cells with persistent knockdown are not discernible without visualizing target gene expression. Although this effect was obvious when targeting three different genes, *GFP*, *RFP*, and *crb*, it is possible that other genes may behave differently. Indeed, we were unsuccessful in observing shadow RNAi cells for three other genes (*fat*, *gigas*, and *dachshund*) in the wing disc using FLP-out Gal4 (Table S1; not shown). While these could represent technical failures, it is also possible that gene-specific factors influence the susceptibility to shadow RNAi, such as transcript/protein expression levels or stability. Similarly, different RNAi reagents may or may not cause shadow RNAi. For both *GFP* and *crb*, we found that an shRNA transgene was much more effective than a long dsRNA transgene in generating shadow RNAi (see Table S1). This difference may simply be explained by better knockdown efficiency using shRNAs compared to dsRNAs, as has been observed previously (Ni *et al.* 2011). Alternatively, shRNAs, which are embedded in a *miR-1* microRNA backbone (Ni *et al.* 2011), might be more stable in cells than long dsRNAs or produce greater numbers of siRNAs. Importantly, it is possible that other hairpin transgenes, derived from different sources or that target different regions of a transcript, may behave differently.

Since shadow RNAi cells can have mutant phenotypes, as we showed with *crb* (Figure 1D), it is important that researchers take this phenomenon into consideration, especially when drawing conclusions about the cell autonomy of mutant phenotypes caused by RNAi-induced knockdown. For some experiments, simply identifying where shadow RNAi cells are located may allow a proper interpretation of results. To test if an shRNA generates shadow RNAi cells *in vivo*, it is critical to visualize target gene expression while conducting knockdown. Although we used antibodies to detect protein levels, *in situ* hybridization to detect transcript levels may also be effective. Complementary to testing an shRNA, a Gal4 line can be assayed with i-TRACE to determine if it causes persistent RNAi of a fluorescent reporter transgene.

We also suggest methods to prevent the generation of shadow RNAi cells. For example, including a temperature-sensitive Gal80 transgene can allow more refined temporal control over when Gal4 is turned on (*e.g.*, Figure 2, C–E), thus giving shadow RNAi cells less time to form. Alternatively, based on our experiments with *GFP* and *crb* knockdown, using long dsRNAs instead of shRNAs seems to prevent formation of shadow RNAi cells. If performing clonal RNAi experiments, we recommend using the MARCM system since this prevents the phenomenon of shadow RNAi clones. Furthermore, shadow RNAi cells are not predicted to occur when using FLP-out Gal4 in nonproliferative tissues since we suggest that transient expression of Gal4 before cell division is required for their generation (Figure 1E).

As an outcome of our work describing RNAi persistence *in vivo*, we developed the i-TRACE system as a novel method to monitor dynamic gene expression from Gal4 reporter lines. The i-TRACE system fills an important gap in existing genetic methods. For example, real-time detection of Gal4 expression is accomplished with a reporter under UAS control (Fischer *et al.* 1988; Brand and Perrimon 1993) but cannot be used to report past expression of Gal4. Conversely, recombination-based methods are used to stably mark cell lineages that previously expressed Gal4 (Evans *et al.* 2009), but can overlook short-term changes in gene expression that occur after stable recombination. The i-TRACE system can be used as a lineage-tracing tool for visualizing recent gene expression, since reporter knockdown in marked cells reverses after ~72 hr. In addition, in at least some situations, the i-TRACE system appears to be a more sensitive reporter of past Gal4 expression than G-TRACE.

Only rarely has a switch in compartment identity been observed near lineage-restricted boundaries, such as in the *Drosophila* embryo (Gettings *et al.* 2010) and in the wing discs during regeneration (Herrera and Morata 2014). Our data demonstrate that cells located at lineage-restricted boundaries of the wing disc can transiently express Gal4 reporters of the opposite compartment identity (Figure 5E), raising the possibility that boundary cells may be less committed to their respective compartmental identities than previously thought, although they ultimately seem to maintain their originally fated compartmental identities. An important caveat is that Gal4 reporter transgenes might not accurately reflect transcription of the endogenous gene. Therefore, it remains unknown whether boundary cells express endogenous identity genes of the opposite compartment and whether this results in transient cell-fate changes. Careful imaging of endogenous compartment identity gene expression in developing wing discs may help resolve this issue. Furthermore, other possibilities such as direct transfer of Gal4 or shRNAs between cells at the boundary also merit consideration.

Acknowledgments

We thank Melanie Worley for discussions and the Bloomington Stock Center, Robert Holmgren, and Norbert Perrimon for fly stocks. This work was supported by grants R01GM61672 and R21EY23924 from the National Institutes of Health and

American Cancer Society Research Professor Award 120366-RP-11-078-01-DDC (to I.K.H.). J.A.B. was funded by the Cancer Research Coordinating Committee of the University of California and T.M.S. was funded by National Science Foundation Graduate Research Fellowship.

Literature Cited

Agaisse, H., U. M. Petersen, M. Boutros, B. Mathey-Prevot, and N. Perrimon, 2003 Signaling role of hemocytes in Drosophila JAK/STAT-dependent response to septic injury. Dev. Cell 5: 441–450.

Alder, M. N., S. Dames, J. Gaudet, and S. E. Mango, 2003 Gene silencing in Caenorhabditis elegans by transitive RNA interference. RNA 9: 25–32.

Baccarini, A., H. Chauhan, T. J. Gardner, A. D. Jayaprakash, R. Sachidanandam *et al.*, 2011 Kinetic analysis reveals the fate of a microRNA following target regulation in mammalian cells. Curr. Biol. 21: 369–376.

Baena-Lopez, L. A., A. Baonza, and A. Garcia-Bellido, 2005 The orientation of cell divisions determines the shape of Drosophila organs. Curr. Biol. 15: 1640–1644.

Bartlett, D. W., and M. E. Davis, 2006 Insights into the kinetics of siRNA-mediated gene silencing from live-cell and live-animal bioluminescent imaging. Nucleic Acids Res. 34: 322–333.

Blair, S. S., 1992 Engrailed expression in the anterior lineage compartment of the developing wing blade of Drosophila. Development 115: 21–33.

Blair, S. S., D. L. Brower, J. B. Thomas, and M. Zavortink, 1994 The role of apterous in the control of dorsoventral compartmentalization and PS integrin gene expression in the developing wing of Drosophila. Development 120: 1805–1815.

Brand, A. H., and N. Perrimon, 1993 Targeted gene expression as a means of altering cell fates and generating dominant phenotypes. Development 118: 401–415.

Brennecke, J., A. A. Aravin, A. Stark, M. Dus, M. Kellis *et al.*, 2007 Discrete small RNA-generating loci as master regulators of transposon activity in Drosophila. Cell 128: 1089–1103.

Buchon, N., N. A. Broderick, S. Chakrabarti, and B. Lemaitre, 2009 Invasive and indigenous microbiota impact intestinal stem cell activity through multiple pathways in Drosophila. Genes Dev. 23: 2333–2344.

Caussinus, E., O. Kanca, and M. Affolter, 2012 Fluorescent fusion protein knockout mediated by anti-GFP nanobody. Nat. Struct. Mol. Biol. 19: 117–121.

Chen, C. L., K. M. Gajewski, F. Hamaratoglu, W. Bossuyt, L. Sansores-Garcia, C. Tao, and G. Halder, 2010 The apical-basal cell polarity determinant Crumbs regulates Hippo signaling in Drosophila. Proc. Natl. Acad. Sci. USA 107: 15810–15815.

Chi, J. T., H. Y. Chang, N. N. Wang, D. S. Chang, N. Dunphy *et al.*, 2003 Genomewide view of gene silencing by small interfering RNAs. Proc. Natl. Acad. Sci. USA 100: 6343–6346.

Croker, J. A., S. L. Ziegenhorn, and R. A. Holmgren, 2006 Regulation of the Drosophila transcription factor, Cubitus interruptus, by two conserved domains. Dev. Biol. 291: 368–381.

Dahmann, C., A. C. Oates, and M. Brand, 2011 Boundary formation and maintenance in tissue development. Nat. Rev. Genet. 12: 43–55.

Dickins, R. A., M. T. Hemann, J. T. Zilfou, D. R. Simpson, I. Ibarra *et al.*, 2005 Probing tumor phenotypes using stable and regulated synthetic microRNA precursors. Nat. Genet. 37: 1289–1295.

Eaton, S., and T. B. Kornberg, 1990 Repression of ci-D in posterior compartments of Drosophila by engrailed. Genes Dev. 4: 1068–1077.

Evans, C. J., J. M. Olson, K. T. Ngo, E. Kim, N. E. Lee *et al.*, 2009 G-TRACE: rapid Gal4-based cell lineage analysis in Drosophila. Nat. Methods 6: 603–605.

Fire, A., S. Xu, M. K. Montgomery, S. A. Kostas, S. E. Driver *et al.*, 1998 Potent and specific genetic interference by double-stranded RNA in Caenorhabditis elegans. Nature 391: 806–811.

Fischer, J. A., E. Giniger, T. Maniatis, and M. Ptashne, 1988 GAL4 activates transcription in Drosophila. Nature 332: 853–856.

Garcia-Bellido, A., P. Ripoll, and G. Morata, 1973 Developmental compartmentalisation of the wing disk of Drosophila. Nat. New Biol. 245: 251–253.

Gettings, M., F. Serman, R. Rousset, P. Bagnerini, L. Almeida *et al.*, 2010 JNK signalling controls remodelling of the segment boundary through cell reprogramming during Drosophila morphogenesis. PLoS Biol. 8: e1000390.

Gupta, S., R. A. Schoer, J. E. Egan, G. J. Hannon, and V. Mittal, 2004 Inducible, reversible, and stable RNA interference in mammalian cells. Proc. Natl. Acad. Sci. USA 101: 1927–1932.

Hafezi, Y., J. A. Bosch, and I. K. Hariharan, 2012 Differences in levels of the transmembrane protein Crumbs can influence cell survival at clonal boundaries. Dev. Biol. 368: 358–369.

Halfon, M. S., H. Kose, A. Chiba, and H. Keshishian, 1997 Targeted gene expression without a tissue-specific promoter: creating mosaic embryos using laser-induced single-cell heat shock. Proc. Natl. Acad. Sci. USA 94: 6255–6260.

Hannon, G. J., 2002 RNA interference. Nature 418: 244–251.

Herrera, S. C., and G. Morata, 2014 Transgressions of compartment boundaries and cell reprogramming during regeneration in Drosophila. eLife 3: e01831.

Hinz, U., B. Giebel, and J. A. Campos-Ortega, 1994 The basic-helix-loop-helix domain of Drosophila lethal of scute protein is sufficient for proneural function and activates neurogenic genes. Cell 76: 77–87.

Kornberg, T., I. Siden, P. O'Farrell, and M. Simon, 1985 The engrailed locus of Drosophila: in situ localization of transcripts reveals compartment-specific expression. Cell 40: 45–53.

Lee, T., and L. Luo, 1999 Mosaic analysis with a repressible cell marker for studies of gene function in neuronal morphogenesis. Neuron 22: 451–461.

Livshits, G., and S. W. Lowe, 2013 Accelerating cancer modeling with RNAi and nongermline genetically engineered mouse models, pp. 991–1005. Cold Spring Harb. Protoc. 2013: pii: pdb.top069856.

Masucci, J. D., R. J. Miltenberger, and F. M. Hoffmann, 1990 Pattern-specific expression of the Drosophila decapentaplegic gene in imaginal disks is regulated by 3′ cis-regulatory elements. Genes Dev. 4: 2011–2023.

McGuire, S. E., P. T. Le, A. J. Osborn, K. Matsumoto, and R. L. Davis, 2003 Spatiotemporal rescue of memory dysfunction in Drosophila. Science 302: 1765–1768.

Micchelli, C. A., and N. Perrimon, 2006 Evidence that stem cells reside in the adult Drosophila midgut epithelium. Nature 439: 475–479.

Mohr, S. E., J. A. Smith, C. E. Shamu, R. A. Neumuller, and N. Perrimon, 2014 RNAi screening comes of age: improved techniques and complementary approaches. Nat. Rev. Mol. Cell Biol. 15: 591–600.

Ni, J. Q., R. Zhou, B. Czech, L. P. Liu, L. Holderbaum *et al.*, 2011 A genome-scale shRNA resource for transgenic RNAi in Drosophila. Nat. Methods 8: 405–407.

Paddison, P. J., A. A. Caudy, E. Bernstein, G. J. Hannon, and D. S. Conklin, 2002 Short hairpin RNAs (shRNAs) induce sequence-specific silencing in mammalian cells. Genes Dev. 16: 948–958.

Pellikka, M., G. Tanentzapf, M. Pinto, C. Smith, C. J. McGlade *et al.*, 2002 Crumbs, the Drosophila homologue of human CRB1/RP12, is essential for photoreceptor morphogenesis. Nature 416: 143–149.

Perrimon, N., J. Q. Ni, and L. Perkins, 2010 In vivo RNAi: today and tomorrow. Cold Spring Harb. Perspect. Biol. 2: a003640.

Phillips, R. G., I. J. Roberts, P. W. Ingham, and J. R. Whittle, 1990 The Drosophila segment polarity gene patched is involved in a position-signalling mechanism in imaginal discs. Development 110: 105–114.

Pignoni, F., and S. L. Zipursky, 1997 Induction of Drosophila eye development by decapentaplegic. Development 124: 271–278.

Richard, M., F. Grawe, and E. Knust, 2006 DPATJ plays a role in retinal morphogenesis and protects against light-dependent degeneration of photoreceptor cells in the Drosophila eye. Dev. Dyn. 235: 895–907.

Roignant, J. Y., C. Carre, B. Mugat, D. Szymczak, J. A. Lepesant *et al.*, 2003 Absence of transitive and systemic pathways allows cell-specific and isoform-specific RNAi in Drosophila. RNA 9: 299–308.

Sijen, T., J. Fleenor, F. Simmer, K. L. Thijssen, S. Parrish *et al.*, 2001 On the role of RNA amplification in dsRNA-triggered gene silencing. Cell 107: 465–476.

Tabata, T., S. Eaton, and T. B. Kornberg, 1992 The Drosophila hedgehog gene is expressed specifically in posterior compartment cells and is a target of engrailed regulation. Genes Dev. 6: 2635–2645.

Tanimoto, H., S. Itoh, P. ten Dijke, and T. Tabata, 2000 Hedgehog creates a gradient of DPP activity in Drosophila wing imaginal discs. Mol. Cell 5: 59–71.

Vaistij, F. E., L. Jones, and D. C. Baulcombe, 2002 Spreading of RNA targeting and DNA methylation in RNA silencing requires transcription of the target gene and a putative RNA-dependent RNA polymerase. Plant Cell 14: 857–867.

Verdel, A., S. Jia, S. Gerber, T. Sugiyama, S. Gygi *et al.*, 2004 RNAi-mediated targeting of heterochromatin by the RITS complex. Science 303: 672–676.

Wilson, R. C., and J. A. Doudna, 2013 Molecular mechanisms of RNA interference. Annu. Rev. Biophys. 42: 217–239.

Xu, T., and G. M. Rubin, 1993 Analysis of genetic mosaics in developing and adult Drosophila tissues. Development 117: 1223–1237.

Yeh, E., K. Gustafson, and G. L. Boulianne, 1995 Green fluorescent protein as a vital marker and reporter of gene expression in Drosophila. Proc. Natl. Acad. Sci. USA 92: 7036–7040.

Zhang, J., C. Wang, N. Ke, J. Bliesath, J. Chionis *et al.*, 2007 A more efficient RNAi inducible system for tight regulation of gene expression in mammalian cells and xenograft animals. RNA 13: 1375–1383.

Zirin, J. D., and R. S. Mann, 2007 Nubbin and Teashirt mark barriers to clonal growth along the proximal-distal axis of the Drosophila wing. Dev. Biol. 304: 745–758.

Zong, J., X. Yao, J. Yin, D. Zhang, and H. Ma, 2009 Evolution of the RNA-dependent RNA polymerase (RdRP) genes: duplications and possible losses before and after the divergence of major eukaryotic groups. Gene 447: 29–39.

Communicating editor: R. J. Duronio

GENETICS

Supporting Information
www.genetics.org/lookup/suppl/doi:10.1534/genetics.116.187062/-/DC1

Persistence of RNAi-Mediated Knockdown in *Drosophila* Complicates Mosaic Analysis Yet Enables Highly Sensitive Lineage Tracing

Justin A. Bosch, Taryn M. Sumabat, and Iswar K. Hariharan

DOI: 10.1534/genetics.116.187062

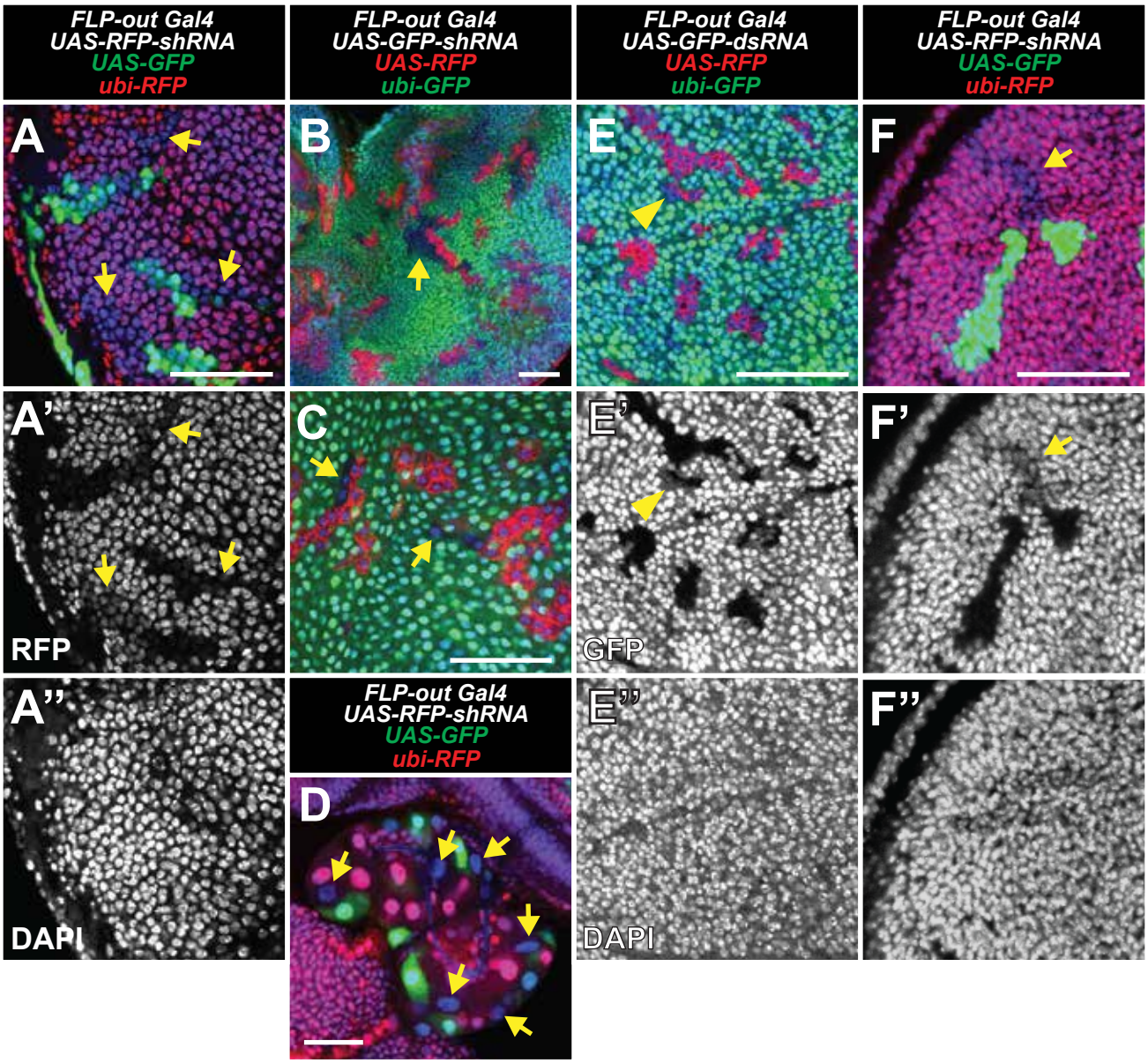

Figure S1. Additional data relevant to Figure 1 (A) Wing imaginal disc with FLP-out clones expressing GFP (green) and *RFP-shRNA*, with knockdown of *ubi-RFP* (red). Arrows indicate shadow RNAi clones. **(B-D)** Larval tissues with shadow RNAi clones, indicated by arrows, **(B)** eye imaginal disc, **(C)** lymph gland, **(D)** prothoracic gland. **(E)** Wing imaginal disc with FLP-out clones expressing RFP (red) and *GFP-dsRNA*, with knockdown of *ubi-GFP* (green). Arrowhead indicates possible shadow RNAi cells. **(F)** Clones induced 72hrs before dissection. Arrow indicates shadow clone. Cell nuclei labeled with DAPI (blue). Scale bars are 50μm.

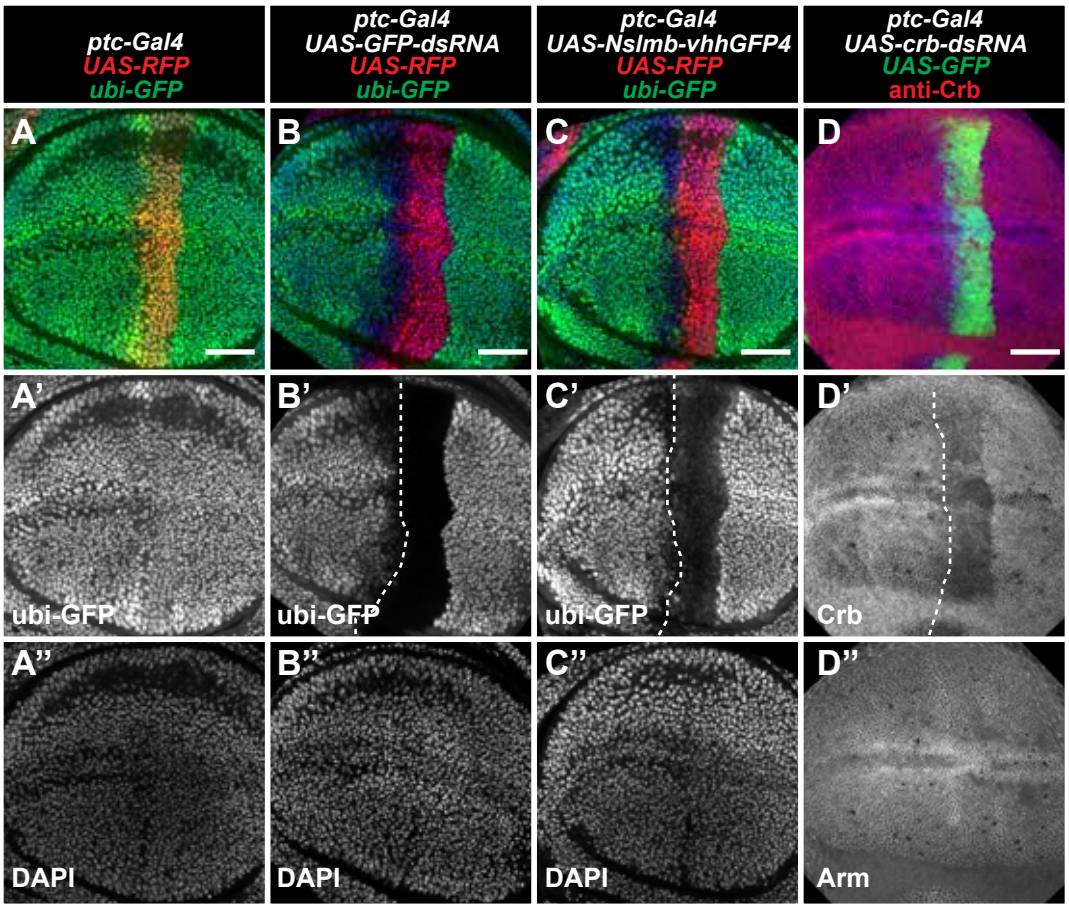

Figure S2. Additional data relevant to Figure 2 (A-D) Wing imaginal discs expressing *ptc-Gal4*. **(A-C)** Expression of RFP (red) in an *ubi-GFP* background. Cell nuclei labeled with DAPI (blue). **(A)** Control disc that does not express *GFP-shRNA*. **(B)** Expression of GFP-dsRNA. **(C)** Expression of Nslmb-vhhGFP4 (deGradFP). vhhGFP4 is a nanobody that binds to GFP protein, and Nslmb is a truncated form of the E3 ubiquitin ligase slmb that contains the F-box domain (Caussinus et al., 2012). Therefore, expression of Nslmb-vhhGFP4 causes ubiquitination of GFP and degradation via the proteasome. **(D)** Expression of GFP (green) and *crb-dsRNA*, and antibody staining for Crb (red). Cell membranes labeled with Arm staining (blue). Scale bars are 50μm.

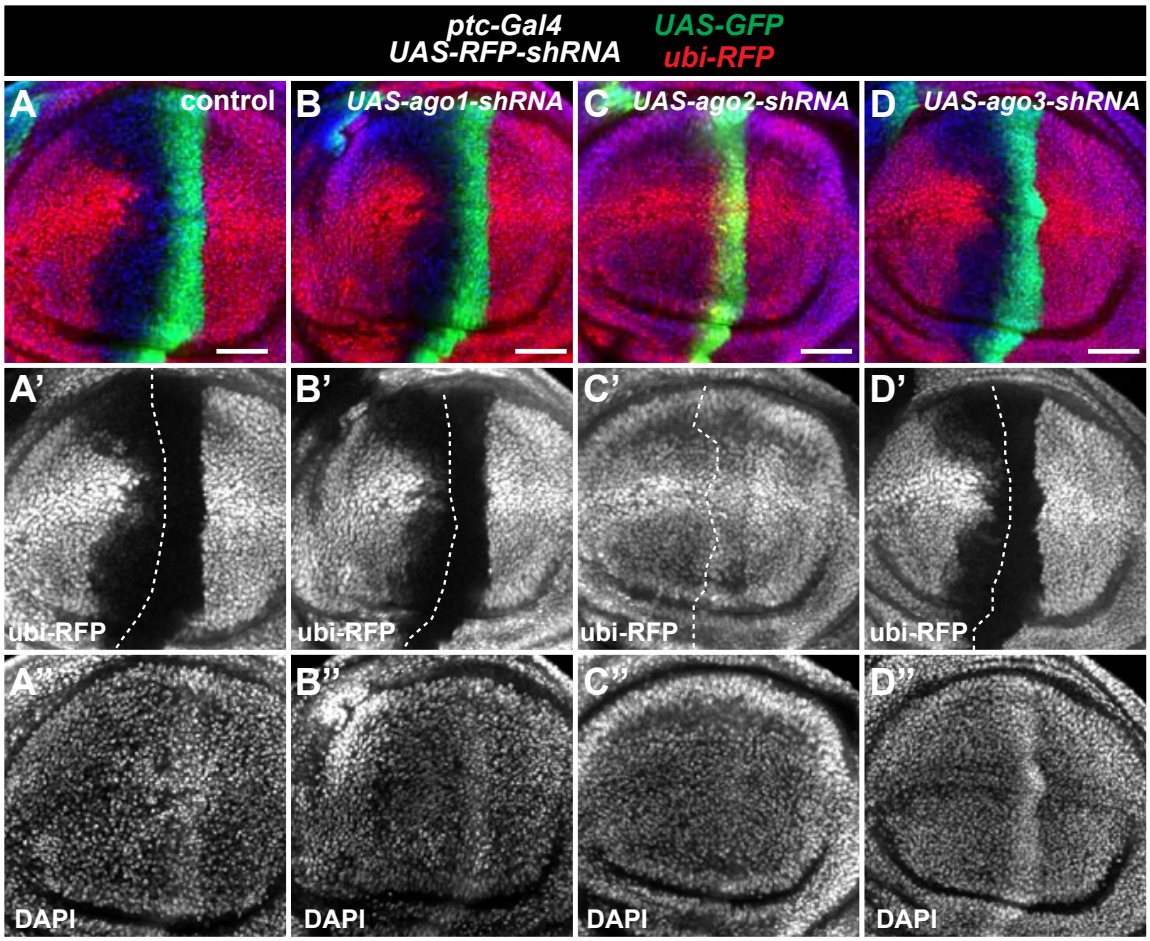

Figure S3. Additional data relevant to Figure 3 (A-D) Wing imaginal disc with *ptc-Gal4* expression of GFP (green) and *RFP-shRNA*, in an *ubi-RFP* background. Cell nuclei labeled with DAPI (blue). **(A)** Control disc. Expression of **(B)** *ago1-shRNA*, **(C)** *ago2-shRNA*, or **(D)** *ago3-shRNA*. Scale bars are 50μm.

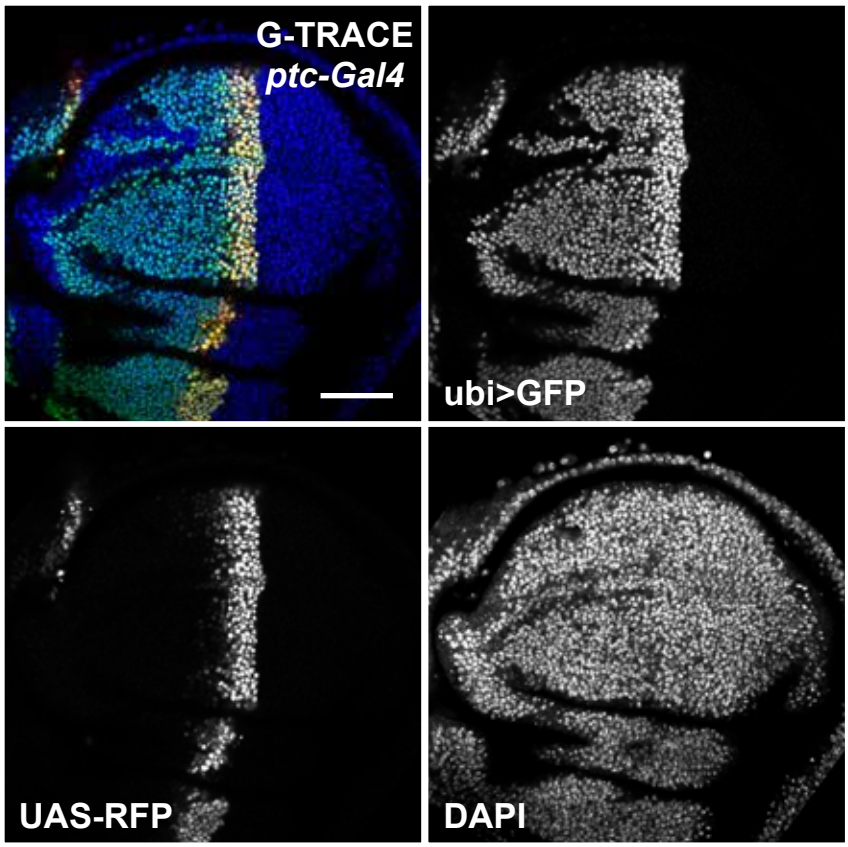

Figure S4. Additional data relevant to Figure 4. G-TRACE analysis of *ptc-Gal4* in the wing imaginal disc. Current expression indicated by RFP (red), recombined lineage expression indicated by GFP (green). Cell nuclei labeled with DAPI (blue). Scale bar is 50μm.

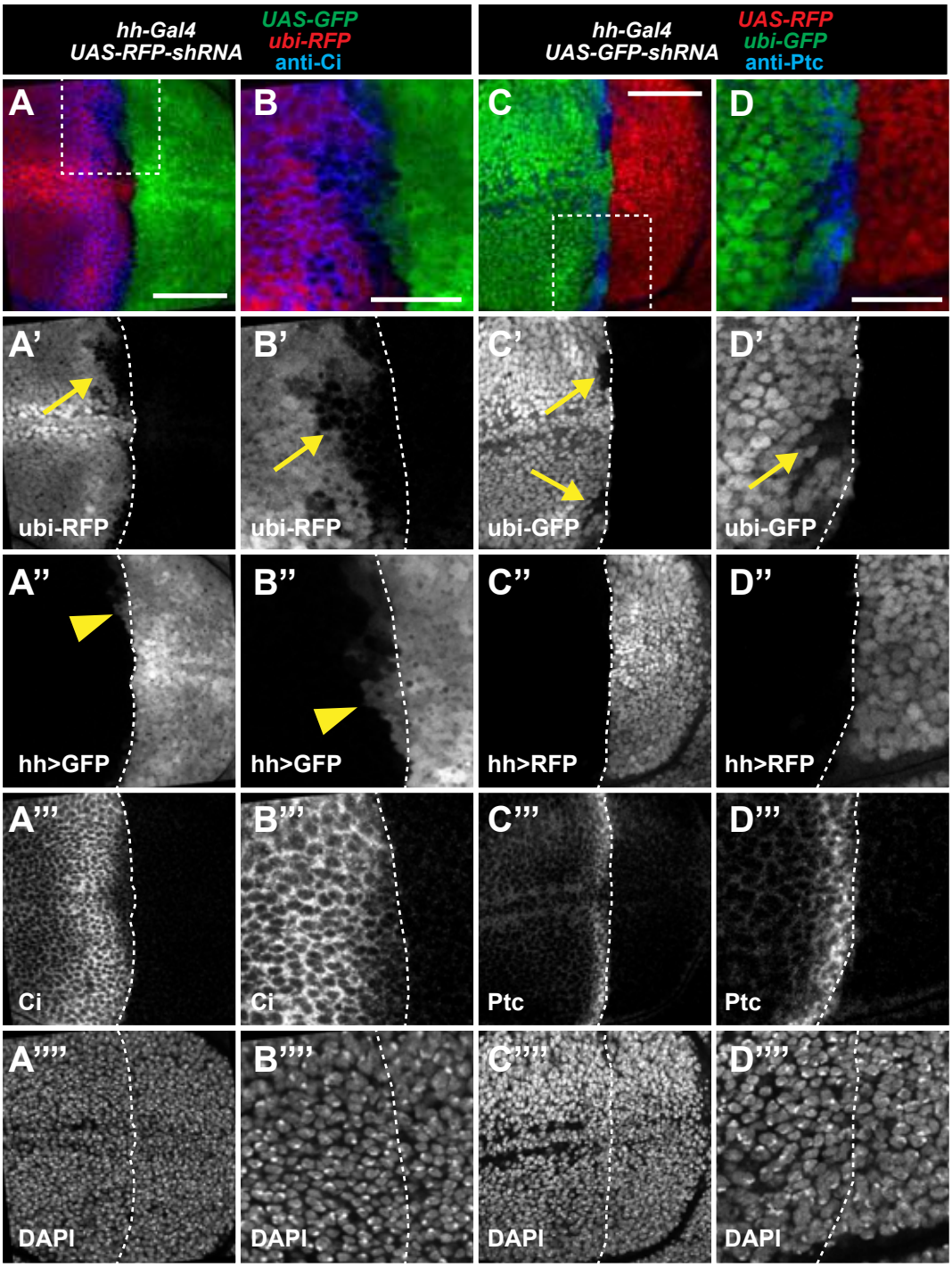

Figure S5. Additional data relevant to Figure 5. Anterior shadow RNAi cells produced from *hh-Gal4* express anterior cell identity markers in the wing imaginal disc. **(A-D)** i-TRACE analysis with *hh-Gal4*. Arrows indicate shadow RNAi cells in anterior compartment. **(A-B)** *hh-Gal4* drives expression of GFP and *RFP-shRNA* in an *ubi-RFP* background. Anti-Ci staining (blue) in the anterior compartment). Arrowheads indicate current expression of *hh-Gal4* in anterior cells. **(B)** Enlargement of box in **A**. **(C-D)** *hh-Gal4* drives expression of RFP and *GFP-shRNA* in an *ubi-GFP* background. Anti-Ptc staining (blue) in anterior cells that border the posterior compartment. **(D)** Enlargement of box in **C**. Scale bars are 50μm in **A** and **C**, and 25μm in **B** and **D**.

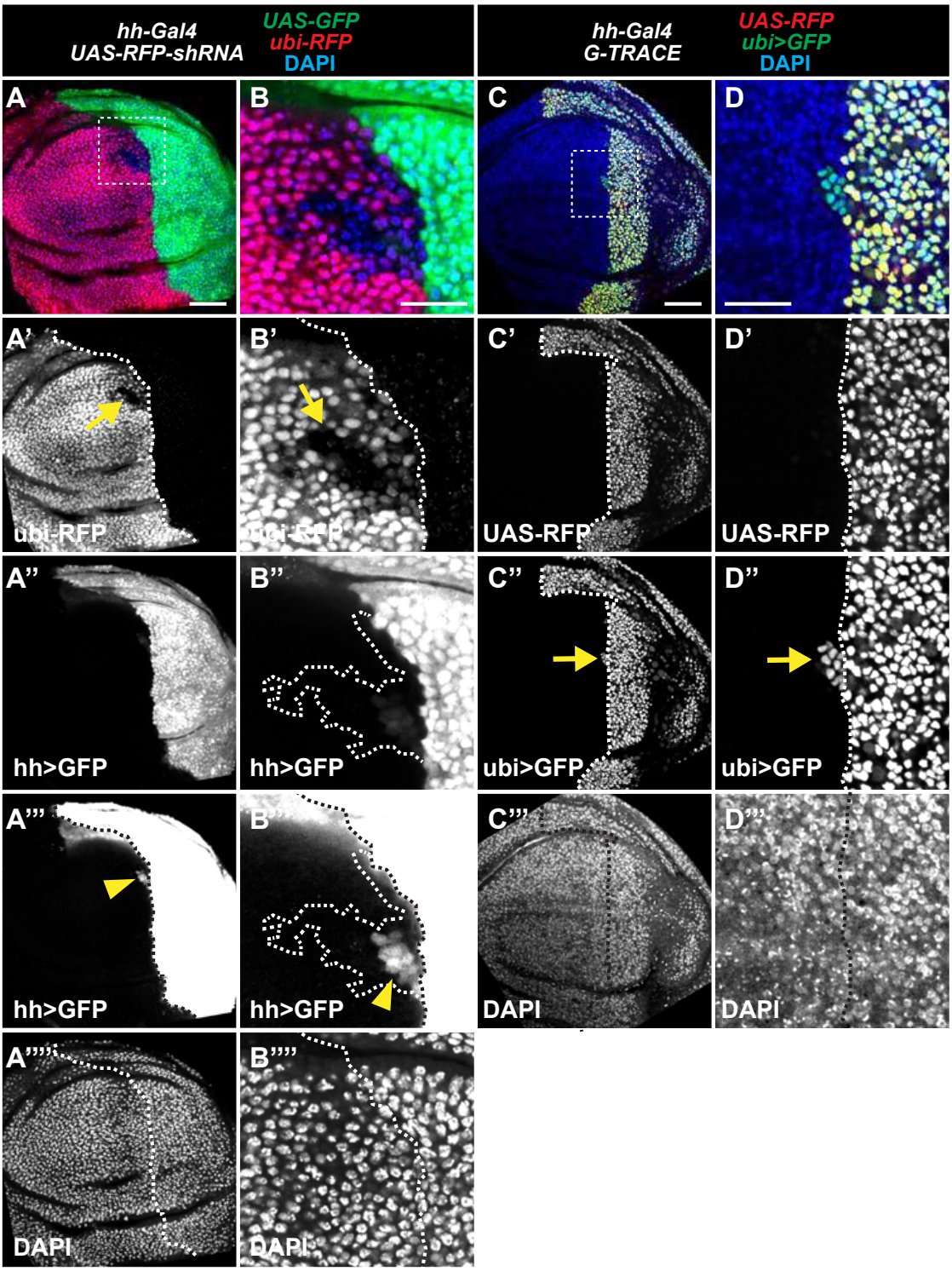

Figure S6. Additional data relevant to Figure 5. (A-B) *hh-Gal4* analyzed with i-TRACE. A subset of cells within anterior shadow RNAi patches exhibit low level current expression of *hh-Gal4*. *hh-Gal4* drives expression of GFP (green) and *RFP-shRNA* in a *ubi-RFP* background. Arrows indicate anterior shadow RNAi cells. Arrowheads indicate anterior cells that currently express *hh-Gal4*. **(B)** Enlargement of box in **A**. The white dotted line in **B''** and **B'''** outlines anterior shadow RNAi cells **(C-D)** *hh-Gal4* analyzed with G-TRACE. RFP marks currently expressing cells, GFP marks past expressing cells. Arrows indicate anterior cells that are GFP+ but RFP-. **(D)** Enlargement of box in **C**. Cell nuclei labeled with DAPI (blue). Scale bars are 50μm in **A** and **C**, and 25μm in **B** and **D**.

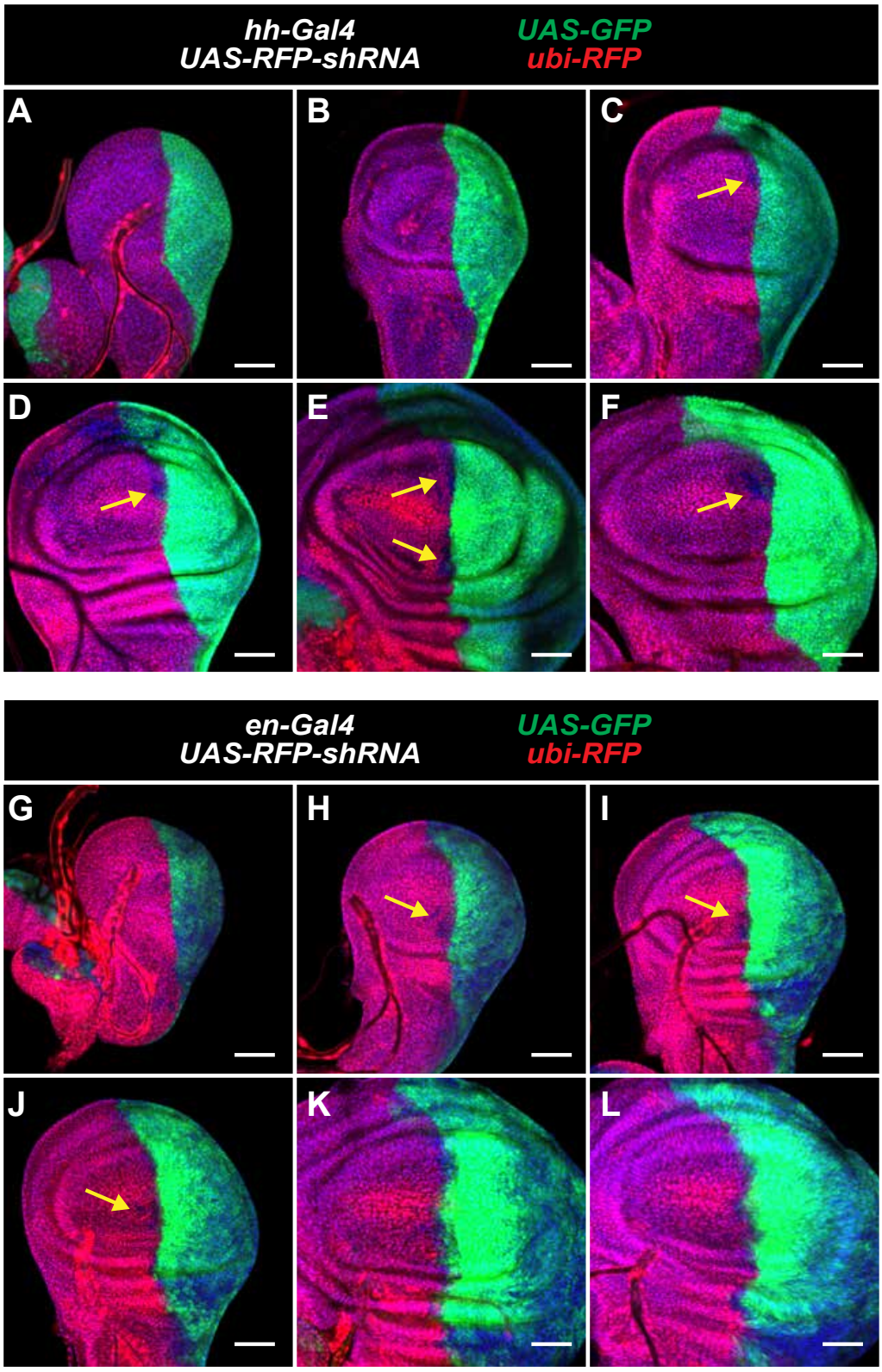

Figure S7. Additional data relevant to Figure 5. Developmental time-series of wing imaginal discs from stages L2 to L3. Arrows indicate shadow RNAi cells. **(A-F)** i-TRACE analysis of *hh-Gal4*. **(G-L)** i-TRACE analysis of *en-Gal4*. **(A-B, G-H)** stage L2 wing discs. **(C-D, I-J)** early stage L3 wing discs. **(E-F, K-L)** late stage L3 wing discs. Cell nuclei labeled with DAPI (blue). All scale bars are 50μm.

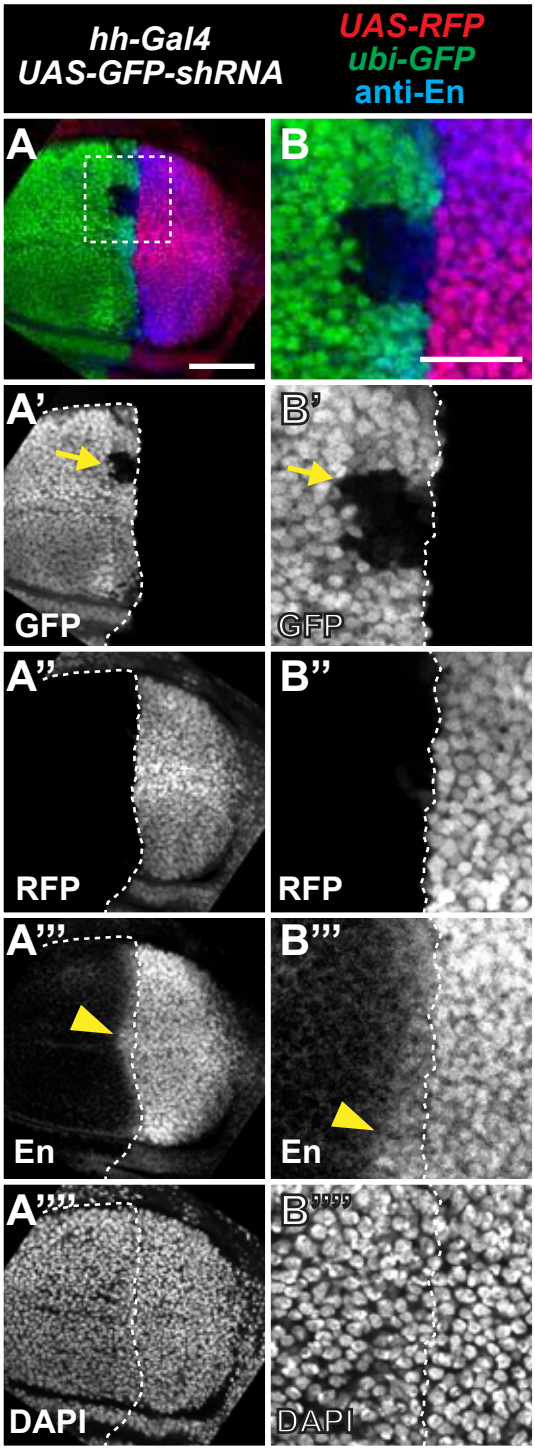

Figure S8. Additional data relevant to Figure 5. Anterior shadow RNAi cells produced from *hh-Gal4* are distinguishable from anterior expression of En in the late 3rd instar wing disc. **(A-B)** i-TRACE analysis with *hh-Gal4*. Arrows indicate shadow RNAi cells in anterior compartment. Arrowheads indicate anterior En expression. **(B)** Enlargement of box in **A**. Cell nuclei labeled with DAPI (blue). Scale bars are 50μm in **A**, and 25μm in **B**.

Target	Knockdown type	Genotype	BL #	FLP-out Gal4 phenotype	Figure	ptc-Gal4 phenotype	Figure
ubi-GFP	dsRNA	w[1118]; P{w[+mC]=UAS-GFP.dsRNA.R}142	9330	rare and faint shadow RNAi cells	Fig. S1	faint shadow RNAi cells anterior to ptc stripe	Fig. S2
ubi-GFP	shRNA	y[1] sc[*] v[1]; P{y[+t7.7] v[+t1.8]=VALIUM20-EGFP.shRNA.1}attP2	41556	obvious shadow RNAi clones	Fig. 1	obvious shadow RNAi cells anterior to ptc stripe	Fig. 2
hs-GFP	shRNA	y[1] sc[*] v[1]; P{y[+t7.7] v[+t1.8]=VALIUM20-EGFP.shRNA.1}attP40	41555	-	-	obvious shadow RNAi cells anterior to ptc stripe	Fig. 3
ubi-GFP	deGradFP	w[*]; P{w[+mC]=UAS-Nslmb-vhhGFP4}3	38421	-	-	faint shadow knockdown cells anterior to ptc stripe	Fig. S2
ubi-RFP	shRNA	y[1] sc[*] v[1]; P{y[+t7.7] v[+t1.8]=VALIUM20-mCherry}attP2	35785	obvious shadow RNAi clones	Fig. S1	obvious shadow RNAi cells anterior to ptc stripe	Fig. S3
crb	dsRNA	y[1] v[1]; P{y[+t7.7] v[+t1.8]=TRiP.JF02777}attP2	27697	-	-	no shadow RNAi cells anterior to ptc stripe	Fig. S2
crb	shRNA	y[1] sc[*] v[1]; P{y[+t7.7] v[+t1.8]=TRiP.HMS02036}attP2	40869	obvious shadow RNAi clones	Fig. 1	obvious shadow RNAi cells anterior to ptc stripe	Fig. 2
gigas	shRNA	y[1] sc[*] v[1]; P{y[+t7.7] v[+t1.8]=TRiP.HMS01217}attP2/TM3, Sb[1]	34737	no shadow clones observed, not in figures	data not shown	-	-
ft	shRNA	y[1] sc[*] v[1]; P{y[+t7.7] v[+t1.8]=TRiP.HMS00932}attP2	34970	no shadow clones observed, not in figures	data not shown	-	-
dac	shRNA	y[1] sc[*] v[1]; P{y[+t7.7] v[+t1.8]=TRiP.HMS01435}attP2	35022	no shadow clones observed, not in figures	data not shown	-	-

Table S1. Summary of genes targeted by RNAi and knockdown transgenes used.

Gene	Function	RNAi Phenotype	Bloomington #	TRiP #	shRNA version
ago1	miRNA associated, RISC component	none	33727	HMS00610	VALIUM20
ago2	siRNA associated, RISC component	Abolishes RNAi of RFP reporter	34799	HMS00108	VALIUM20
ago3	piRNA pathway	none	34815	HMS00125	VALIUM20
eIF-2gamma	S. pombe RITS homologue	none	33401, 32914	HMS00279, HMS00704	VALIUM20
Su(var)3-9	S. pombe RITS homologue	none	33401, 32914	HMS00279	VALIUM20
HP1c	S. pombe RITS homologue	none	33962	HMS00919	VALIUM20
G9a	S. pombe RITS homologue	none	34817	HMS00127	VALIUM20
Trf4-1	S. pombe RITS homologue	none	41966	HMS02363	VALIUM20
pic	S. pombe RITS homologue	none	33888	HMS00826	VALIUM20
Su(var)205 (HP1)	Heterochromatin	none	33400	HMS00278	VALIUM20
Pc	Polycomb-group protein	none	33622	HMS00016	VALIUM20
Psc	Polycomb-group protein	none	38261	HMS01706	VALIUM20
pho	Polycomb-group protein	none	42926	HMS02619	VALIUM20

Table S2. Additional data relevant to Figure 3 and Supplemental Figure 3 Genes targeted by RNAi to test their requirement for RNAi persistence. Each RNAi line was crossed with a tester line that contains the following transgenes: *ptc-Gal4, UAS-GFP, UAS-GFP-shRNA, ubi-RFP*. Wing discs were imaged to determine if the pattern of RFP RNAi is altered. Ago2 RNAi abolishes RFP RNAi in all cells, but other RNAi lines tested do not alter the pattern of RFP RNAi in the wing disc (see Figure S3).